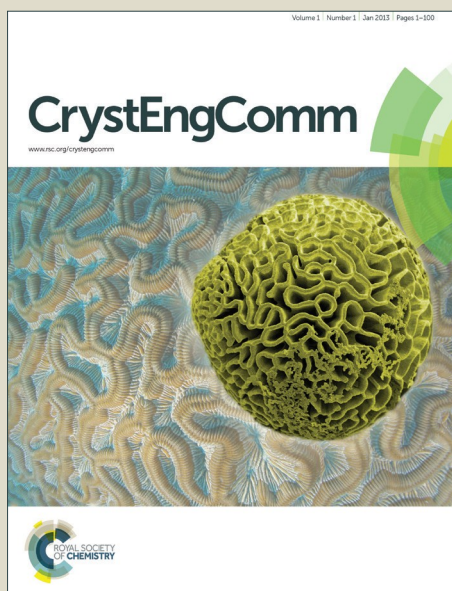


CrystEngComm

Accepted Manuscript



This article can be cited before page numbers have been issued, to do this please use: L. Zhang, Z. Kang, X. Xin and D. Sun, *CrystEngComm*, 2015, DOI: 10.1039/C5CE01917F.



This is an *Accepted Manuscript*, which has been through the Royal Society of Chemistry peer review process and has been accepted for publication.

Accepted Manuscripts are published online shortly after acceptance, before technical editing, formatting and proof reading. Using this free service, authors can make their results available to the community, in citable form, before we publish the edited article. We will replace this *Accepted Manuscript* with the edited and formatted *Advance Article* as soon as it is available.

You can find more information about *Accepted Manuscripts* in the [Information for Authors](#).

Please note that technical editing may introduce minor changes to the text and/or graphics, which may alter content. The journal's standard [Terms & Conditions](#) and the [Ethical guidelines](#) still apply. In no event shall the Royal Society of Chemistry be held responsible for any errors or omissions in this *Accepted Manuscript* or any consequences arising from the use of any information it contains.

ARTICLE

Metal-organic frameworks based luminescent materials for Nitroaromatics sensing†

Cite this: DOI: 10.1039/x0xx00000x

Liangliang Zhang,† Zixi Kang,† Xuelian Xin, Daofeng Sun*

Received 00th January 2012,
Accepted 00th January 2012

DOI: 10.1039/x0xx00000x

www.rsc.org/

Metal-organic frameworks (MOFs), composed of organic ligands and metal nodes, are well known for their high and permanent porosity, crystalline nature and versatile potential applications, which promoted them to be one of the most rapidly developing research focuses in chemical and material science. During the various applications of MOFs, the photoluminescence properties of MOFs have received growing attention, especially for the nitroaromatics (NACs) sensing, due to the consideration of homeland security, environmental cleaning and military issues. In this highlight, we summarize the recent research progress in NACs sensing based on LMOFs cataloged by sensing technique in the last three years, and then we describe the sensing applications on nano-MOF type materials and MOF film, together with MOF film applications.

Introduction

With the increasing use of explosive materials in terrorism all over the world, how to reliably and efficiently detect tracing explosive materials has become a highlight research focus in recent years because of homeland security, environmental cleaning and military issues.¹ Additionally, the reliable identification of chemical explosives in post-blast residues is of great important for criminal investigations.^{1d,2} As one of major classes of secondary explosives, nitroaromatics (NACs), which are composed of a benzene ring functionalized with several nitro-groups, have become serious pollution sources of groundwater, soils, and other security applications due to their explosivity and high toxicity, such as 2,4,6-trinitrotoluene (TNT), 2,4-dinitrotoluene (2,4-DNT) and picric acid (PA) (Fig. 1). The detection of this class of explosives is not easy because of their moderate vapor pressures and limited chemical reactivity.^{1e} Thanks to the development of instrumental techniques together with sniffer dogs,³ new ways to detect

explosives are being developed to improve security, including gas chromatography coupled with mass spectrometry (GC-MS), surface-enhanced Raman spectroscopy, neutron activation analysis, X-ray imaging, ion mobility spectroscopy (IMS), energy dispersive X-ray diffraction (EDXRD), plasma desorption mass spectrometry (PDMS) and so on.^{1k,4} These techniques are highly selective and sensitive, but some are of high cost and time-consuming, simultaneously others are not easy to operate and be assembled in a small and low-power package. Therefore, another new technology need to be developed so that we may cheaply and rapidly complete detection. The electron-deficient particular property of NACs is favorable for forming π -stacking complexes with electron-rich fluorophores, which can be applied to their detection with chromo-fluorogenic probes. Chemical sensors provide new approaches to the rapid detection of ultra-trace NACs from explosives, and can be easily incorporated into inexpensive and portable microelectronic devices. In this respect, the

fluorescence-based sensor schemes probably show a very promising future.

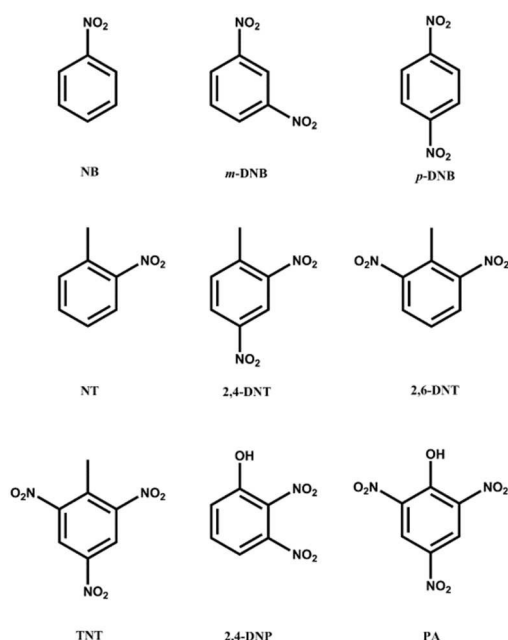


Fig. 1 Chemical structures of common NACs molecules.^{1f}

All sorts of conjugated polymers (CPs) have been used to sensing NACs with high sensitivity and selectivity, due to their π -electron-rich characteristic and high binding strength to NACs.^{1i, 5} The delocalized π^* excited state of the CPs can significantly enhance their donor ability and enable them to interact strongly with nitrated aromatic compounds through π - π interactions. However, the applications of conjugated polymeric sensors are limited for their stability, multi-step synthesis and poor molecular organization. In addition, it has also been noted that porosity may play an important role in the sensing performance, as illustrated in porous amplifying fluorescent polymer (AFP) films, metalloporphyrin-doped mesostructured films and fluorescent nanofibril films.

Metal-organic frameworks (MOFs) materials, constructed from multi-topic organic ligands and metal cations or clusters, have been extensively studied during the past decade for their intriguing structural diversity and potential applications including selective gas adsorption and separation,⁶ catalysis,⁷ luminescent sensing^{3a, 8} and drug delivery.⁹ MOFs have become

one of the most rapidly developing research focuses in chemical and materials sciences. The most attractive features of MOFs are their high and permanent porosity, long range order, high surface area, as well as uniform pore sizes in the nanoscale range. Additionally, the chemical versatility and structural tailorability provide a significant level of tenability to the physical and chemical properties of MOFs. The judicious combination of metal ions and predesigned organic ligands under suitable reaction conditions affords various kinds of MOF structures with desired functionalities.¹⁰ The luminescence of MOFs originates from the rigid ligands with aromatic moieties or extended π systems and/or metal components especially for lanthanides and inorganic clusters, excimer and exciplex, or guest molecules. Compared with free organic ligand, the advantages of using MOFs as sensory materials are as follows. At first, MOFs in solid may reduce the non-radiative decay rate and leads to increased fluorescence intensity, lifetimes, and quantum efficiencies. In addition, the multifunction of MOFs can easily be modulated by post-synthetic modification and it is supposed that unsaturated metal centers or open metal sites plays important part in absorption/separation including gas and guest molecules. Most notably, the sustainable pores within LMOFs provide a natural habitat for guest molecules. The combination of porosity and luminescence in MOFs makes them potential candidates for the sensing of NACs. After reported by Li in 2009, the fluorescence based sensing materials have recently been considered as one of the most excellent and promising techniques in the detection of NACs.^{1c}

The possible mechanisms of luminescent MOFs for sensing NACs are based on fluorescent quenching, including an electron transfer or energy transfer process, or a combination of the two between fluorophore and NACs, and the similar physical process have been investigated in conjugated polymers.^{2, 3c, 11} The fluorescent quenching mechanism based on electron transfer can also be divided into static quenching and dynamic quenching. The static quenching takes place in the

ground-state via non-fluorescent electron-transfer complex formation, which decreases the intensity of steady-state emission, without changing the life-time of LMOFs. On the contrary, the dynamic quenching occurs in the excited state with electron-transfer process, which decreases the steady-state emission intensity and life-time of LMOFs simultaneously. As mentioned above, NACs are electron-deficient analytes and LMOFs can be regarded as electron-rich fluorophore molecules, whose valence and conduction bands can be treated in the similar way of molecular orbitals (MOs). The vapor pressure and reduction potential of common explosives and selected analytes are listed in Table 1. The electronic properties of LMOFs and NACs are equally important for efficient sensing. In general, the conduction of a LMOFs lies at higher energies than the LUMOs of NACs, and thus maintains a better driving force for the electron transfer to electron-deficient NACs, leading to the fluorescent quenching. Stern-Volmer analysis can be used to evaluate the efficiency of particular LMOFs for NACs in liquid medium quantitatively using Equation(1).

$$I_0/I_f = 1 + k_{sv}[Q], \quad \text{Equation(1)}$$

Where I_0 and I_f are the fluorescent intensities of LMOFs before and after the addition of NACs. k_{sv} is Stern-Volmer constant and $[Q]$ stands for the concentration of NACs. The higher k_{sv} means high sensing efficiency. But the electron transfer is not the sole mechanism, the fluorescent quenching mechanism sometime originates from the case of energy transfer or the combination of electron and energy transfer. If the emission band of LMOFs and the absorption band of the NACs are efficiently overlapped, the energy transfer process may occur and will severely improve the fluorescence quenching

efficiency and sensibility. The probability of resonance energy transfer depends on the extent of spectral overlap between the emission of LMOFs and the absorption of NACs. The extent of energy transfer was determined by calculating the integral of overlap (J_λ) values using Equation(2).¹² Where, $F_D(\lambda)$ is the corrected fluorescence intensity of donor in the range of λ to $\lambda + \Delta\lambda$ with the total intensity normalized to unity, and ϵ_A is extinction coefficient of the acceptor at λ in $M^{-1} cm^{-1}$.

$$J(\lambda) = \int_0^\infty F_D(\lambda)\epsilon_A(\lambda)\lambda^4 d\lambda \quad \text{Equation(2)}$$

The advantages and challenges of LMOFs based on chemical sensing and explosive detection have been well summarized by recent review articles.^{1f, 8b, 8c, 11, 13} Our research interest focus on NACs sensing based on LMOFs. In this highlight, we summarize the recent research progress in NACs sensing based on LMOFs cataloged by sensing technique in the last three years, and then we describe the sensing applications on nano-MOF type materials and MOF film, together with MOF film applications.

Table 1 The vapor pressure of common NACs

Analyte	Vapor pressure (in mmHg, ^a at 25 °C)
Nitrobenzene (NB)	0.2416
1,3-Dinitrobenzene (<i>m</i> -DNB)	8.82×10^{-4}
1,4-Dinitrobenzene (<i>p</i> -DNB)	2.406×10^{-5}
2-Nitrotoluene (NT)	0.1602
2,4-Dinitrotoluene (2,4-DNT)	1.44×10^{-6}
2,6-Dinitrotoluene (2,6-DNT)	5.61×10^{-4}
2,4,6-Trinitrotoluene (TNT)	8.02×10^{-6}
Picric acid (PA)	5.8×10^{-9}

^a1 mmHg = 1.2468 × 103 ppm.

Table 2 List of selected LMOFs in recent three years.

LMOFs	Solvent	Sensing	λ_{ex} (nm)	λ_{em} (nm)	ref
[Zn(L ¹)(dpb)]	EtOH	Liquid phase	310	415	14
[Zn(L ²)(dpb)]	EtOH	Liquid phase	300	420	14
[Zn(L ³)(dpb)]	EtOH	Liquid phase	360	480	14
[Zn ₂ (NDC) ₂ (bpy)]·G _x	EtOH	Liquid phase	320	450	1m
Zn(L ⁴)-(HDMA) ₂ (DMF)(H ₂ O) ₆	EtOH	Liquid phase	Not	475	15

$\{[Zn_2(PIA)_2(bpy)_2] \cdot 2.5H_2O \cdot DMA\}_n$	EtOH	Liquid phase	280	326	16
$[Cd(fdc)(bpee)_{1.5}] \cdot 3(H_2O)$	EtOH	Liquid phase	300	425	17
$[Cd_3(CPEIP)_2(DMF)_3] \cdot \text{solvent}$	EtOH	Liquid phase	342	Not given	18
$[Cd_2Cl(tba)_3] \cdot 0.5DMF \cdot 2H_2O$	EtOH	Liquid phase	323	381	19
$[Cd_3(TPT)_2(DMF)_2] \cdot (H_2O)_{0.5}$	EtOH	Liquid phase	333	390	20
$[La(TPT)(DMSO)_2] \cdot H_2O$	EtOH	Liquid phase	342	374	21
$Eu_2(BDC)_3(H_2O)_2$	EtOH	Liquid phase	315	617	22
$[Tb(HL^5)(H_2O)_4] \cdot H_2O$	EtOH	Liquid phase	288	546	23
$\{[Tb_2(TATAB)_2] \cdot 4H_2O \cdot 6DMF\}_n$	EtOH	Liquid phase	350	545	24
Tb(BTC)	EtOH	Liquid phase	353	548	25
$[Tb(TTCA)(DMA)(H_2O)] \cdot 7DMA \cdot 9.5H_2O$	EtOH	Liquid phase	370	540	26
$[Zn_2(L^1)(L^2)(dpb)_2]$	EtOH	Liquid phase	330	417	27
$[Zn_2(L^1)(L^3)(dpb)_2]$	EtOH	Liquid phase	347	471	27
$[Zn_2(L^2)(L^3)(dpb)_2]$	EtOH	Liquid phase	350	476	27
$[Zn_3(L^1)(L^2)(L^3)(dpb)_3]$	EtOH	Liquid phase	350	473	27
$[Zn_3(TDPAT)(H_2O)_3]$	MeOH	Liquid phase	370	435	28
$[Zn_4(OH)_2(1,2,4-BTC)_2]$	MeOH	Liquid phase	331	428	29
$[Zn_4O(L^6)_3(DMF)_2] \cdot 0.5DMF \cdot H_2O$	MeOH	Liquid phase	280	380	30
$(NH_2Me_2)_6[In_{10}(TTCA)_{12}] \cdot 24DMF \cdot 15H_2O$	MeOH	Liquid phase	410	505	31
$[Zn(PAM)(en)]$	DMSO	Liquid phase	371	503	32
$[Cd_2(PAM)_2(dpe)_2(H_2O)_2] \cdot 0.5(dpe)$	DMSO	Liquid phase	371	502	33
$[Eu(L^7)(H_2O)(NMP)] \cdot 1.5H_2O$	DMSO	Liquid phase	298	616	34
$[Tb_3(NO_3)(BPTA)_2(H_2O)_6] \cdot 3Diox \cdot 8H_2O$	DMSO	Liquid phase	330	545	11
$\{Li_3[Li(DMF)_2](CPMA)_2\} \cdot 4DMF \cdot H_2O$	DMF	Liquid phase	345	430	35
$[NH_2(CH_3)_2][Mg_3(NDC)_2.5(HCO_2)_2(DMF)_{0.75}(H_2O)_{0.25}]$	DMF	Liquid phase	340	380	36
$[Zn_7O_2(bpdc)_4(dmpp)_2] \cdot 6DEF \cdot 10H_2O$	DMF	Liquid phase	323	390	37
$[Zn_2(bpeb)(sdb)_2]$	DMF	Liquid phase	360	453	38
$[Zn_2(fdc)_2(bpee)_2(H_2O)]_n \cdot 2H_2O$	DMF	Liquid phase	350	425	39
$[(Zn_4O)(DCPB)_3] \cdot 11DMF \cdot 5H_2O$	DMF	Liquid phase	330	354	40
$(CH_3)_2NH_2Zn_3(HL^8)(H_2O)_2] \cdot 4H_2O$	DMF	Liquid phase	374	443	41
$[NH_2Me_2]_4[Cd_3(H_2L^9)]$	DMF	Liquid phase	348	446	42
$[Cd_3(TCA)_4(H_2O)_2]$	DMF	Liquid phase	352	417	43
$[NH_2(CH_3)_2][Cd_{17}(L^{10})_{12}(H_2O)_4(DMF)_2(H_2O)_2]$	DMF	Liquid phase	290	360	44
$[Cd_8(D-cam)_8(bimb)_4]_n$	DMF	Liquid phase	370	410	45
$[Cd(TPTZ)(H_2O)_2(HCOOH)(IPA)_2]$	DMF	Liquid phase	360	450	46
$[Cd_3(TTPB)_2(H_2O)_6] \cdot 6DMF$	DMF	Liquid phase	366	440	47
$[NH_2(CH_3)_2][Cd_6(L^{10})_4(DMF)_6(HCOO)]$	DMF	Liquid phase	290	353	48
$Eu_3(MFDA)_4(NO_3)(DMF)_3$	DMF	Liquid phase	336	615	49
$(Me_2NH_2)_3[Eu_3(MHFDA)_4(NO_3)_4(DMF)_2] \cdot 4H_2O \cdot 2MeCN$	DMF	Liquid phase	340	614	50
$[Eu_2(MFDA)_2(HCOO)_2(H_2O)_6]$	DMF	Liquid phase	335	614	51
$[Ln(L^{11})_{1.5}(DEF)]_n$	DMF	Liquid phase	340	615	52
$[In_2L^{12}][NH_2(CH_3)_2]_2 \cdot (DMF)_4(H_2O)_{16}$	DMF	Liquid phase	280	360	53
$Cd(L^4) \cdot (NH_2Me_2)_2(DMF)(H_2O)_3$	acetonitrile	Liquid phase	330	460	15
$Zn(L^4) \cdot (NH_2Me_2)_2(DMF)(H_2O)_6$	acetonitrile	Liquid phase	330	452	15
$Mg_5(OH)_2(BTEC)_2(H_2O)_4 \cdot 11H_2O$	THF	Liquid phase	328	425	54
PCN-224		Liquid phase	590	651	55

[Zn ₂ (L ¹³) ₂ (dpyb)]	DMA	Liquid phase	382	533	56
[Zn(L ¹³)(dipb)]·(H ₂ O) ₂	DMA	Liquid phase	382	523	56
{[Cd ₂ L ¹⁴ (H ₂ O) ₂]·DMF·H ₂ O} _n	DMA	Liquid phase	290	401	57
[Cd(L ¹⁵) _{0.5} (H ₂ O)]·H ₂ O	DMA	Liquid phase	350	414	58
[Cd ₂ Cl(H ₂ O)(L ¹⁶)]·4.5DMA	DMA	Liquid phase	295	377,390,474	59
[Cd ₃ (NTB) ₂ (DMA) ₃]·2DMA	DMA	Liquid phase	366	443	60
[CdCl(L ¹⁷)Eu(H ₂ O)(DMA)]·(NO ₃) ₃ ·3DMA	DMA	Liquid phase	367	671	61
{[Zn ₃ (μ-OH) ₂ (SDB) ₂]·(PPZ)} _n	Acetone	Liquid phase	270	292	62
{[Cd(SDB)(H ₂ O)]·3H ₂ O} _n	Acetone	Liquid phase	270	290	62
[Eu ₃ (bpydb) ₃ (HCOO)(OH) ₂ (DMF)]·(DMF)·3(H ₂ O) ₂	DMF and H ₂ O	Liquid phase	362	615	63
[Cd(H ₂ ttac)bpp] _n	DMF and ethanol	Liquid phase	320	415	64
[Zn ₂ (L ¹⁸)(bipy)(H ₂ O) ₂]·(H ₂ O) ₃ (DMF) ₂	MeCN	Liquid phase	350	476	65
Cd(L ⁴)·(HDMA) ₂ (DMF)(H ₂ O) ₃	MeCN	Liquid phase	Not	460	15
[Cd(NDC) _{0.5} (PCA)]·Gx	MeCN	Liquid phase	340	384	12a
[Mg ₂ (BDC) ₂ (BPNO)]·2DMF		Vapor phase	305	421	66
[Zn _{1.5} (L ¹⁹)(H ₂ O)]·1.5benzene		Vapor phase	280	390	67
[Zn ₂ (TCPPE)]		Vapor phase	365	461	68
[Zn ₂ (oba) ₂ (bpy)]·3DMA		Vapor phase	280	420	1g
[Zn ₂ (bpd) ₂ (bpee)]·2DMF		Vapor phase	320	422	1c
[Zn(ndc)(bpy) _{0.5}]		Vapor phase	300	450	69
[Zn(ndc)(bpe) _{0.5}]		Vapor phase	330	425	69
[Zn(ndc)(bpee) _{0.5}]		Vapor phase	330	450	69
[Zn(ndc)(ted) _{0.5}]		Vapor phase	340	420	69
[Zn(dcbpy)(DMF)]·DMF		Vapor phase	Not	Not given	70
[Dy(dcbpy)(DMF) ₂ (NO ₃)]		Vapor phase	Not	Not given	70
[Zn ₈ (ad) ₄ (BPDC) ₆ O·2Me ₂ NH ₂]·G(G = DMF and water)	H ₂ O		340	405	71
[(CH ₃) ₂ NH ₂] ₃ [Zn ₄ Na(BPTC) ₃]·4CH ₃ OH·2DMF	H ₂ O		295	360	72
[Cd(ppvppa)(1,4-NDC)] _n	H ₂ O		419	478	3b
[Eu(BTB)H ₂ O]	H ₂ O		350	610	73
{[Tb(L ²⁰) _{1.5} (H ₂ O)]·3H ₂ O}	H ₂ O		329	541	74
[Tb(L ²¹)(OH)]·x(solvent)	H ₂ O		350	541	75
[Tb(BTB)H ₂ O]	H ₂ O		350	541	73
Zr ₆ O ₄ (OH) ₄ (L ²²) ₆	H ₂ O		395	500	76
Zr ₆ O ₄ (OH) ₄ (L ²⁴) ₆	H ₂ O		320	450	77
Ur-MOF	H ₂ O		310	390	78

applied to detecting NACs with high selectivity and sensitivity in vapor phase, liquid phase and/or aqueous phase. The results show that LMOFs are kinds of promising materials to trace the nitroaromatic explosives.

2.1 Detection in vapor phase

Gas sensors have a wide range of application in the fields of aerodynamics, environmental analysis, analytical chemistry, and biochemistry. As the luminescent properties of MOFs can

2 MOFs for NACs sensor

As a new frontier for material research, Metal-organic frameworks (MOFs) have gathered numerous attentions in the last decades, due to their multi-functional applications. A brand new field of MOF research which associated with NACs detection was represented after firstly reported by Li etc. Among the reported studies, MOFs or hybrid MOFs were

also be perturbed by gases and vapors, some luminescent MOFs for sensing of gases and vapors have been also explored.^{3a, 11} The very first MOF used as sensor in vapor phase to detect NACs explosives was reported by Li's group.^{1c} They designed and synthesized a fluorescent MOF, $[\text{Zn}_2(\text{bpdc})_2(\text{bpee})] \cdot 2\text{DMF}$ (bpdc = 4,4'-biphenyldicarboxylate; bpee = 1,2-bipyridylethene; DMF = dimethyl formamide). The MOF consisted of 1D open channels, in which DMF molecules were filled in, and the solvent molecules could be removed by heating under vacuum to obtain the guest-free MOF. The guest-free MOF showed strong fluorescence in solid state. To explore the applicability for detecting the NACs, the guest-free MOF was made as thin layer. The sample showed rapid and reversible response to DNT vapor, the quenching percentage reached 85% within 10 seconds. Thus, it is important that the samples can detect DNT circularly by heating the samples at 150 °C for one minute. Moreover, Li's group also reported a Zn based LMOF, LMOF-121 or $[\text{Zn}_2(\text{oba})_2(\text{bpy})] \cdot \text{DMA}$, H_2oba = 4,4'-oxybis-(benzoic acid), bpy = 4, 4'-bipyridine, DMA = *N,N*-dimethylacetamide).^{1g} As shown in Fig. 2, LMOF-121 possessed a 3D network built from a $\text{Zn}_2(\text{oba})_4$ paddle-wheel SBU. The structure contained one-dimensional open 1D channels running along both the 100 and 010 directions, where the DMA molecules resided. To obtain the empty pore for capturing the guest molecule, LMOF-121 was heating at 160 °C to remove DMA molecules, as LMOF-121'. The fluorescent spectra of LMOF-121' was carried in thin layer, which showed strong emission at 420 nm (λ_{ex} = 280 nm). The layer was exposed to different NACs with electron withdrawing groups. The results indicated that all the NACs used in the article acted as fluorescent quenchers. The quenching efficiency (%) of NB was 84% which was the highest one (Fig.3). In the vapor phase, the quenching efficiency is not only affected by the strong electron-withdrawing $-\text{NO}_2$ group, but also associated with the vapor pressure. Recently, the same group reported a series of fluorescence active MOFs built on paddle-wheel secondary building units (SBUs), including $[\text{Zn}(\text{ndc})(\text{bpe})_{0.5}]$ (**1**),

$[\text{Zn}(\text{ndc})(\text{bpee})_{0.5}]$ (**2**), $[\text{Zn}(\text{ndc})(\text{ted})_{0.5}]$ (**3**) and $\text{Zn}(\text{ndc})(\text{bpy})_{0.5}$ (**4**) [ndc = 2,6-naphthalenedicarboxylic acid; bpe = 1,2-bis(4-pyridyl)-ethane; bpee = 1,2-bis(4-pyridyl)-ethylene; ted = triethylenediamine, bpy = 4,4' -bipyridine]. All compounds performed luminescent quenching when they are exposed to the NACs vapor. Among them, complex **3** possesses the best quenching ability, with the quenching ratio about 84% and 51% for NB and NT vapor respectively.⁶⁹ The similar results can be observed in Wang,⁶⁶ and Shen's⁶⁸ work.

LMOFs can also be synthesized via microwave assisted method, because it sharply reduces the over-all processing time, increases the product yield and improves the quality of the product. Compared to their solvothermally synthesised counterparts, microwave-assisted LMOFs with homogenous microcrystals give increased sensing sensitivities. Parkin and coworkers reported two fluorescent metal-organic frameworks $[\text{Zn}(\text{dcbpy})(\text{DMF})] \cdot \text{DMF}$ (**1**) and $[\text{Dy}(\text{dcbpy})(\text{DMF})_2(\text{NO}_3)]$ (**2**) (dcbpy = 2,2'-bipyridine-4,4'-dicarboxylate), together with microwave synthesized form, as **1M**. Microporous **1** and nonporous **2** give organic linker-based fluorescence emission. And then MOFs **1**, **1M** and **2** were tested for their ability to act as sensory materials to TNT derivatives: 2,4-dinitrotoluene (2,4-DNT), para-nitrotoluene (*p*-NT) and nitrobenzene (NB), as well as plastic explosive taggant 2,3-dimethyl-2,3-dinitrobutane (DMNB) in vapor phase. They demonstrated very different detection capabilities towards the explosive taggant. Compared with non-homogenous microcrystals of **1**', **1M** shows greater sensitivities of quenching responses when exposed to DMNB and NB. They believe that the differences are attributed to the variation in the overall framework architecture between the two MOFs. This paper reiterates the key importance of MOF porosity in sensing applications, and highlights the value of uniform microcrystals to sensitivity.⁷⁰

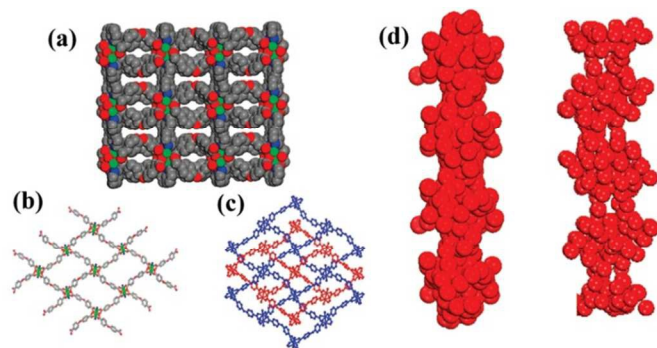


Fig. 2 Crystal structure of $[\text{Zn}_2(\text{oba})_2(\text{bpy})]\cdot\text{DMA}$. (a) Space-filling model of the 3D framework, showing the 1D channels running along the 100 direction without DMA molecules. (b) A single layer (Zn, green; N, blue; O, red). (c) Twofold interpenetration, shown by two different colors (blue and red). (d) The atom filling in a single channel along the (left) 010 and (right) 100 direction. Reprinted with permission from ref 1g. Copyright American Chemistry Society 2011.

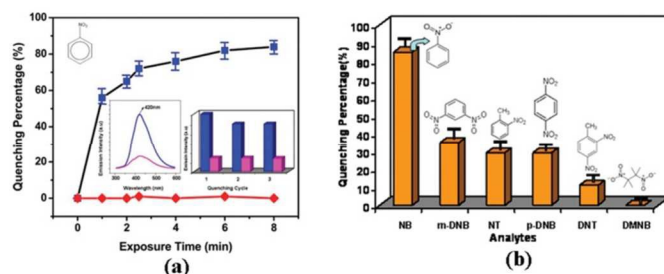


Fig. 3 (a) Time-dependent fluorescence quenching by NB (black line) and DMNB (red line). Insets: (left) corresponding emission spectra before and after exposure of LMOF-121' to the NB vapor; (right) results for three continuous quenching cycles. (b) Percentage of fluorescence quenching after 15 min by five different analytes at room temperature. Reprinted with permission from ref 1g. Copyright American Chemistry Society 2011.

2.2 Detection in liquid phase

In recent years, most LMOFs for NACs sensors are detected in organic liquid phase, including EtOH, MeOH, DMF, DMA, DMSO and MeCN, especially for unstable MOFs. Our group has reported an example of MOFs as efficient sensor for NACs detection.³⁴ $[\text{Eu}_2(\text{L}^7)_2(\text{H}_2\text{O})_3]\cdot 2\text{H}_2\text{O}$ ($\text{H}_3\text{L}^7 = 1,3,5\text{-tris}(4\text{-carboxyphenyl-1-ylmethyl-2,4,6-trimethylbenzene})$) was crystallized in orthorhombic, space group of $Pnma$. As showed in Fig. 4(a)-(d), the binuclear Eu clusters are connected to each

other by two carboxylate groups to form 1D infinite rod-shaped SBU along the c axis. The 1D chain is further linked by ligands to form a porous 3D MOF, which contains a rhombic channel viewed from the c axis. The detection of various NACs was tested. The fluorescent quenching percentage was showed in Fig. 4(e) and (f), and the number is up to 75% for NP at the concentration being 0.13 mM in DMSO solution. The results showed that the OH^- group in NP, which possible interacts apparently with the emission through electrostatic interactions. As a continue of our research, we also reported a Tb based MOF, $[\text{Tb}_3(\text{NO}_3)(\text{BPTA})_2(\text{H}_2\text{O})_6]\cdot 3\text{Diox}\cdot 8\text{H}_2\text{O}$ (**UPC-11**, $\text{H}_4\text{BPTA} = [1,1'\text{-biphenyl}]-2,2',5,5'\text{-tetracarboxylic acid}$, Diox = 1,4-dioxane), which could rapidly and selectively detect NACs. The MOF exhibits luminescent emissions at 290, 545, 584 and 622 nm with the excitation at 330 nm, those peaks are tentatively assigned to $^5\text{D}_4 \rightarrow ^7\text{F}_6$, $^5\text{D}_4 \rightarrow ^7\text{F}_5$, $^5\text{D}^4 \rightarrow ^7\text{F}_4$, $^5\text{D}^4 \rightarrow ^7\text{F}_3$ transitions of Tb^{3+} ion. The luminescent titration show that all NACs can weaken the fluorescence intensity of **UPC-11** suspension, but the quenching percentage exhibits a big difference. Meanwhile, the addition of 1,3-DNB, 2,4-DNT, 1,4-DNB, 4-NA, 1-M-4-NB, and 4-NPH solution caused relatively little but similar fluorescent intensity change of suspension, but the introduction of 4-NP produced significant quenching of fluorescence intensity. **UPC-11** shows rapid and selective fluorescent sensing properties of NACs, especially for 4-nitrophenol (NP).¹¹

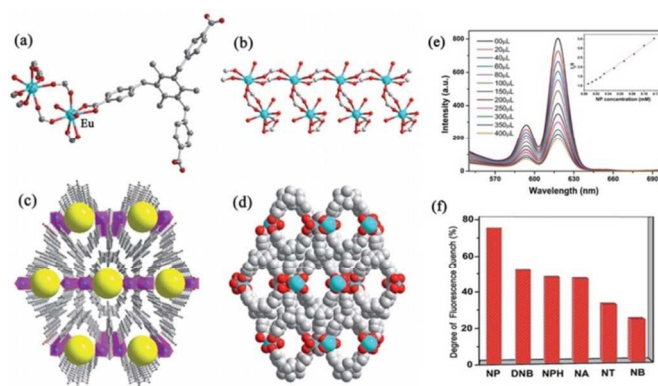


Fig. 4 (a) Coordination environment of Eu atom in $[\text{Eu}_2(\text{L}^7)_2(\text{H}_2\text{O})_3]\cdot 2\text{H}_2\text{O}$. (b) The 1D rod shaped SBU in

ARTICLE

[Eu₂(L⁷)₂(H₂O)₃]-2H₂O. (c) Projection view of the framework [Eu₂(L⁷)₂(H₂O)₃]-2H₂O along the c axis. (d) 3D porous framework shown in the space-filling mode. (e) Effect on the emission spectra of [Eu₂(L⁷)₂(H₂O)₃] dispersed in DMSO upon incremental addition of a NP DMSO solution (1 mM). The legend indicates the overall concentration of NP. The Stern–Volmer plot of I_0/I versus the NP concentration is shown in the inset. (f) The degree of fluorescence quenches upon the addition of the nitrobenzene derivatives (0.13 mM). Reprinted with permission from ref 34. Copyright the Royal Society of Chemistry 2015

Nitroaromatic explosives with different numbers of –NO₂ groups can be detected in qualitative and quantitative according to Lan and Su's report.⁷⁹ They present a luminescent Ln³⁺@MOF approach to realize a fast and effective Ln³⁺@MOF sensor used to detect nitroaromatic explosives with high recyclability through fluorescence quenching. And the concentrations of complete quenching are about 2000, 1000, and 80 ppm for nitro-benzene, 1,3-dinitrobenzene, and 2,4,6-trinitrophenol, respectively. Meanwhile, to examine the sensing sensitivity toward TNP in more detail, a batch of suspensions of Tb³⁺@NENU-522 were prepared by dispersing it in a DMF solution while gradually increasing the contents to monitor the emissive response. Tb³⁺@NENU-522 displays high selectivity and recyclability in the detection of nitroaromatic explosives. The group also reported NENU-503 for quick and sensitive detection of nitroaromatic explosives through fluorescence quenching.⁵⁹ Notably, the detection of TNT by the MOF can be easily distinguished by the naked eye (Fig. 5). This fluorescence quenching is ascribed to photo-induced electron transfer and resonance energy transfer. For the first time, a MOF can distinguish between NB, 1,3-DNB, and TNP with different numbers of NO₂ groups by the shift of the PL spectra. High stability and recyclability of NENU-503 make it an outstanding candidate in the field of detection of explosives.

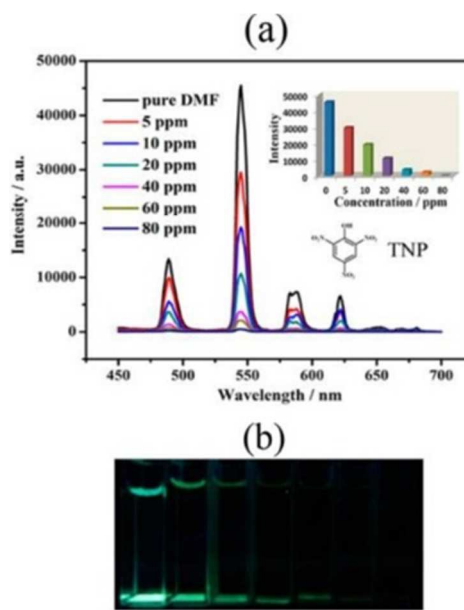


Fig. 5 (a) Emission spectra of Tb³⁺@NENU-522 in different concentrations TNP in DMF (excited at 333 nm). Inset: Corresponding emission intensities. (b) Corresponding emission intensities of Tb³⁺@NENU-522 in different concentrations of TNP in DMF. Reprinted with permission from ref 59. Copyright American Chemistry Society 2015.

2.3 Detection in both vapor and solution phase

The detection of NACs can also be operated both in vapor and solution phase. Lu's group reported a 3D luminescent microporous MOF with 1D channels based on triphenylene-2,6,10-tricarboxylate, (Me₂NH₂)₆[In₁₀(TTCA)₁₂]-24DMF·15H₂O (TTCA = triphenylene-2,6,10-tricarboxylate and DMF = N,N'-dimethylformamide)³¹. The framework is of anionic and Me₂NH₂²⁺ cations decomposed from DMF are filled in the channels to balance the charge. The photoluminescence spectrum of framework exhibits strong emission at 505 nm with excitation at 410 nm. The maximum fluorescent intensity of sample was reduced by 41.7, 62.1, 73.5, and 65.9% upon exposure to 2 mM methanol solutions of TNT, 2,4-DNT, 2,6-DNT, and NB, respectively. The compound shows selective sensing of the nitro explosive TNP, making it a promising sensing material for TNP monitoring.

Chen's group developed a fluorescent In based MOF, [In₂L¹²][NH₂(CH₃)₂]₂·(DMF)₄(H₂O)₁₆ (DMF = N,N'-

dimethylformide, H_8L^{12} = tetrakis[(3,5-dicarboxyphenoxy)methyl]methane with a (4,8)-connected *scu* topology (Fig. 6). $[In_2L^{12}][NH_2(CH_3)_2]_2 \cdot (DMF)_4 \cdot (H_2O)_{16}$ exhibited a strong fluorescent emission at 360 nm ($\lambda_{ex} = 280$ nm) at room temperature. On one hand, in vapor phase, the MOF dispersed in DMF was exposure to different concentration ($mol \cdot L^{-1}$) of several NACs. The fluorescent intensity reduced by 81.5% of 5×10^{-6} mol/L NB is the most efficient (Fig. 7). The excellent fluorescence quenching response to NACs is due to the electrostatic interactions between the MOF and the electron-deficient NACs. The quenching response is associated with both the electron-withdrawing groups of NACs and the sizes of the pore in MOF. On the other hand, the samples were immersed into DMF solution and several analytes ($0.5 mol \cdot L^{-1}$) were added into the solution. The NACs show inefficient quenching, and the quenching mechanism is similar to those reported by Li's group before.⁵³

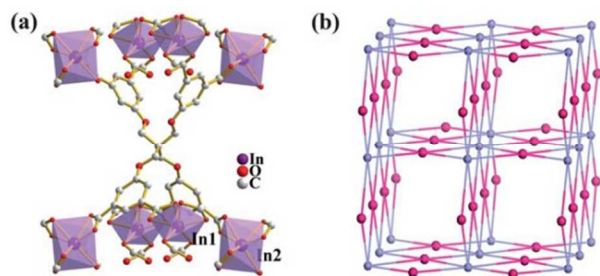


Fig. 6 Views of (a) the organic ligand which is connected to eight In atoms; (b) the resulting 4,8-connected framework with *scu* topology, and structures viewed along. Reprinted with permission from ref 53. Copyright The Royal Society of Chemistry 2013.

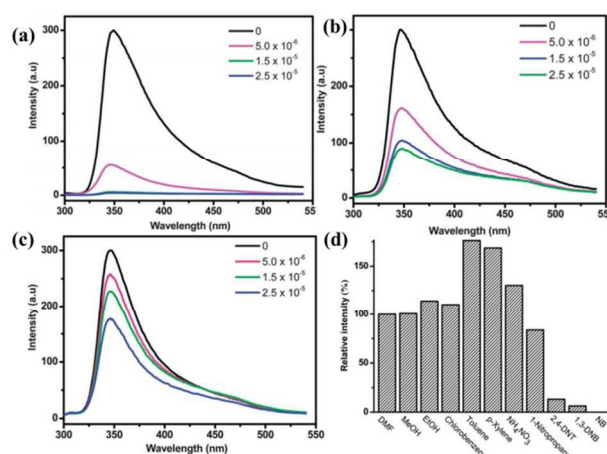


Fig. 7 Quenching response before and after exposure to different concentrations ($mol L^{-1}$) of (a) NB, (b) 1,3-DNB, and (c) 2,4-DNT in DMF solution for 2 min ($\lambda_{ex} = 280$ nm). d) Percentage of fluorescence quenching or enhancement after the samples were immersed into different analytes ($0.5 mol L^{-1}$) in DMF for 2 min at room temperature (excited at 280 nm). Reprinted with permission from ref 53. Copyright The Royal Society of Chemistry 2013.

In Zhang's work, a multi-responsive sensor with a red-emission signal is successfully obtained by the solvothermal reaction of Eu^{3+} and heterofunctional ligand $bpydbH_2$ (4,4'-(4,4'-bipyridine-2,6-diyl) dibenzoic acid), followed by terminal-ligand exchange in a single-crystal-to-single-crystal transformation. It can discriminate among the homologues and isomers of aliphatic alcohols and detect highly explosive 2,4,6-trinitrophenol (TNP) in water or in the vapor phase, which may contribute to the electrostatic interactions between free Lewis-base sites and hydroxyl groups in analytes.⁶³

Konar and coworkers reported a 2D Cu(I)-based MOF, $[Cu(L)(I)]_{2n} \cdot 2nDMF \cdot nMeCN$ (**1**); $L^{23} = 4'-(4\text{-methoxyphenyl})-4,2':6',4''\text{-terpyridine}$; DMF = *N,N'*-dimethylformamide, MeCN = acetonitrile (Fig. 8), which seems to be the first report of any material which reversibly encapsulates explosive nitroaromatics in vapor phase in single crystal to single crystal fashion with visible color changes without loss of framework integrity (Fig. 9). The MOF also represents one of the best hosts reported so far having extreme stability and selectivity

that meets the benchmark of reversibility for material applications.⁸⁰

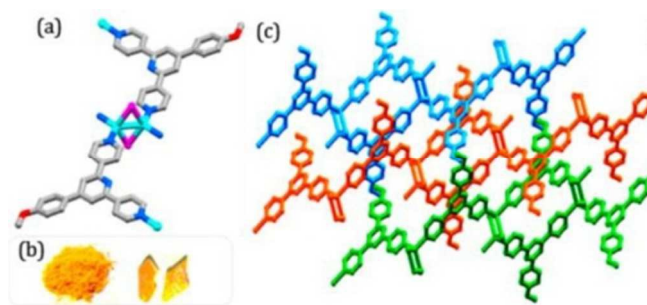


Fig. 8 (a) Illustration of $[\text{Cu}_2\text{L}^{23}]$ as secondary building unit (SBU) and its extension through ligands (L^{23}). (b) Color of the powder form and crystals of the as-synthesized complex. (c) 3D interdigitated structure showing three neighboring layers in three different colors. Reprinted with permission from ref 80. Copyright the American Chemistry Society 2015.

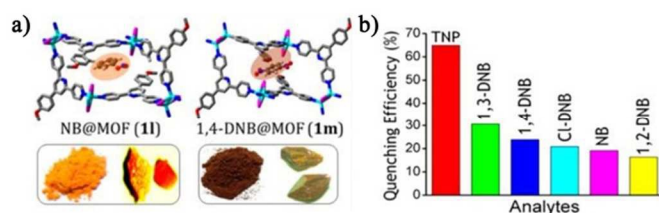


Fig. 9 Illustration of guest exchange with visible color changes in NB and 1,4-DNB vapors. (b) Fluorescence quenching efficiency for different analytes in MeCN solution. Reprinted with permission from ref 80. Copyright the American Chemistry Society 2015.

Hou and Zang have reported a highly fluorescent MOF $\{[\text{Tb}(\text{L}^{21})(\text{OH})] \cdot x(\text{solv})\}$ under a combination of hydro/solvothermal and ionothermal conditions.⁷⁵ The fluorescence of that MOF shows high selectivity and sensitivity towards the presence of trace amounts of nitroaromatic analytes in both aqueous and vapor phases, probably through a redox quenching mechanism similar to that in conjugated polymer systems. The origin of the highly selective sensing towards nitroaromatic explosives can be attributed to a photo-induced electron transfer from MOF to nitroaromatic explosives. Further analysis demonstrates that TNP can efficiently quench the fluorescence of the MOF via both electron and long range

energy transfer processes, while other nitroaromatic explosives quench the fluorescence by an electron transfer process only.

2.4 Detection in aqueous phase

In actuality, the detection of nitroaromatics in an aquatic system is highly desirable for practical applications. Ghosh reported a fluorescent porous Zr(IV) based MOF $\text{Zr}_6\text{O}_4(\text{OH})_4(\text{L}^{24})_6$ (**1**, UiO-67@N, H_2L^{24} = 2-phenylpyridine-5,4'-dicarboxylic acid) demonstrate highly selective and sensitive detection of TNP in aqueous media even in the presence of competing nitro analytes (Fig. 10). The guest free MOF was dispersed in water and exhibited strong fluorescence upon excitation at 320 nm. To explore the changes of fluorescence intensity when the different nitro aromatic compounds like TNP, TNT, 2,4-DNT, 2,6-dinitrotoluene (2,6-DNT), 1,3-dinitrobenzene (DNB), NB and 1,3,5-trinitro-1,3,5-triazacyclohexane (nitro-amine RDX) was added. With the incremental addition of TNP to **1**' resulted in fast and high fluorescence quenching (73%) (Fig. 11). Fluorescence quenching can be clearly observed for TNP concentrations of as low as 2.6 mM. At low TNP concentrations a linear increase in the SV plot was observed, which upon and the fitting of the SV plot for TNP gave a quenching constant of $2.9 \times 10^4 \text{ M}^{-1}$, which is amongst the highest values known for MOFs. The occurrence of both electron and energy transfer processes, in addition to electrostatic interaction between the MOF and TNP, contribute to the unprecedented selective fluorescence quenching.⁷⁷ They also reported a hydrolytically stable 3D luminescent metal-organic framework, $[\text{Zn}_8(\text{ad})_4(\text{BPDC})_6\text{O} \cdot 2\text{Me}_2\text{NH}_2] \cdot \text{G}$ (G = DMF and water). The compound in water exhibited a strong emission at 405 nm ($\lambda_{\text{ex}} = 340 \text{ nm}$). The emission spectra were recorded by fluorescence titration with different NACs, such as TNP, TNT, 2,4-DNT, and 2,6-DNT. The results showed fast detection and high fluorescence quenching (93 %) for TNP. The MOF can sense TNP at extremely low concentrations, with a detection limit of 12.9 nM.⁷¹ Recently, the same group developed a highly selective and sensitive aqueous phase

detection of NACs, such as 2,4,6-trinitrophenol (TNP) by a water-stable, porous luminescent metal–organic framework, $[\text{Zn}_4(\text{DMF})(\text{Ur})_2(\text{NDC})_4]$ (NDC = 2,6-naphthalenedicarboxylic acid, Ur = urotropin, DMF = *N,N'*-dimethylformamide).⁷⁸

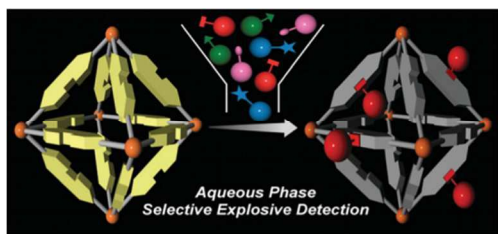


Fig. 10 A fluorescent MOF based sensor for highly selective nitro explosive detection in the aqueous phase. Reprinted with permission from ref 77. Copyright The Royal Society of Chemistry 2014.

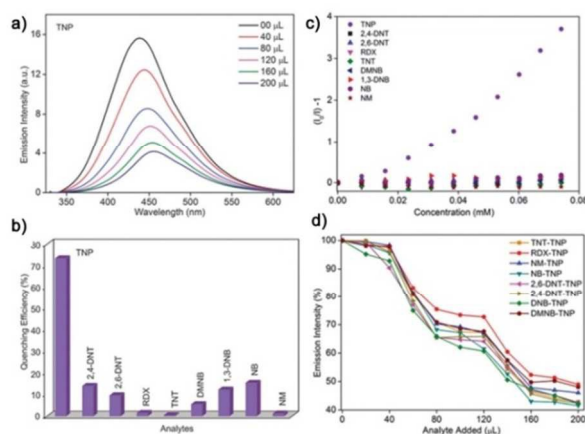


Fig. 11 The change in the fluorescence intensity in water upon incremental addition of aqueous 1 mM TNP solution ($\lambda_{\text{ex}} = 320$). (b) The fluorescence quenching efficiency for different analytes; (c) Stern–Volmer (SV) plots for various NACs in water. (d) The decrease in fluorescence intensities upon the addition of various nitro analytes (1 mM) followed by TNP (1 mM) in aqueous media. Reprinted with permission from ref 77. Copyright The Royal Society of Chemistry 2014.

Ionic liquids (ILs) assisted synthesis of MOFs have received increasing attention because their strong polarity improving the reaction conditions of crystalline materials. Hou and Zang group reported two novel lanthanide metal–organic frameworks (Ln-MOFs) $[\text{Ln}(\text{BTB})\text{H}_2\text{O}]$ via ionic liquids method, where Ln = Eu **1**, Tb **2**. **1** and **2** are isostructural and consist of infinite

rod-shaped lanthanide-carboxylate building units which are further bridged by trigonal-planar BTB ligands to give noninterpenetrated open 3D frameworks. The fluorescence properties of **1** and **2** were investigated in water emulsions at 293 K. **1** and **2** both show high selectivity and sensitivity towards the presence of trace amounts of nitroaromatic analytes in the aqueous phase. The emission response was monitored by fluorescence titration with NB, TNP, and 2-NT. The fluorescence quenching efficiency of **1** and **2** increased drastically with the analyte (NB, TNP, and 2-NT). The quenching efficiency can be quantitatively explained by the Stern–Volmer equation, and the calculated K_{sv} values for NB, 2-NT, and TNP were 6.17×10^{-2} , 2.87×10^{-2} , and 6.76×10^{-2} ppm⁻¹ for **1**, and 7.54×10^{-2} , 7.46×10^{-2} , and 3.25×10^{-2} ppm⁻¹ for **2**, respectively. The fluorescence response mechanism might be attributed to the photo-induced electron transfer from the excited MOF to the electron deficient analytes adsorbed on the particle surface of **1** and **2**.⁷³ Su and Qin group reported a stable luminescent anionic metal–organic framework $[(\text{CH}_3)_2\text{NH}_2]_3\{\text{Zn}_5\text{Na}_2(\text{BPTC})_4\}_n \cdot 4\text{CH}_3\text{OH} \cdot 2\text{DMF}$, which showed highly selective detection of TNP in aqueous solution, which can be attributed to electron transfer mechanisms as well as energy transfer mechanisms.⁷²

2.5 Detection with hybrid MOFs

Qiu have reported a rational self-sacrificing template strategy to obtain tubular nanostructures based on MOF-type materials, and have demonstrated their application for trace-level detection of nitroaromatic explosives. The resultant fluorescent MOFNTs have proven fast, highly sensitive and selective, and reversible for trace-level detection of nitroaromatic explosives, clearly demonstrating that such fluorescent tubular MOF nanostructures can serve as an ideal candidate for fast detection of nitro explosives (Fig. 12).⁸¹

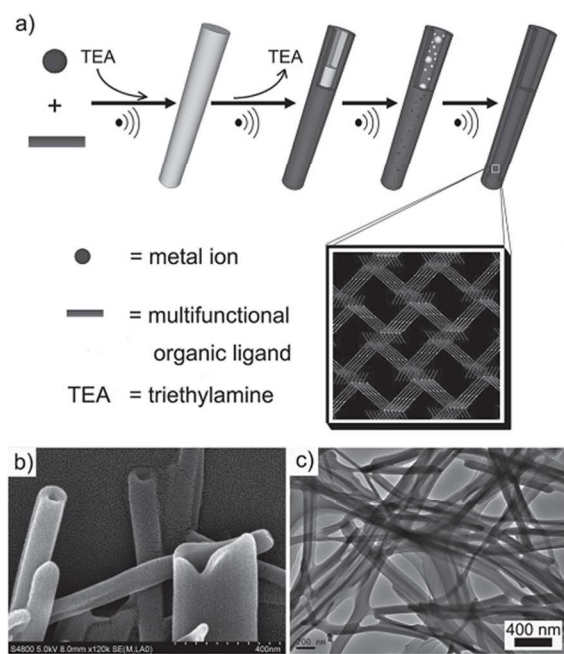


Fig. 12 (a) Illustration of the fabrication process of MOFNTs by the self-sacrificing template strategy. (b) Close-up SEM image of open-ended MOFNTs. (c) Representative TEM image of MOFNTs. Reprinted with permission from ref 81. Copyright the Royal Society of Chemistry 2014.

The same group also successfully fabricated $[\text{Tb}(\text{BTC})]_n$ nanocrystals by a combined ultrasound-vapour phase diffusion method.²⁵ The nanoscale Tb-based MOFs exhibit excellent luminescence properties for the highly selective and sensitive detection of PA, and no obvious interference from other nitroaromatic compounds such as NB, 2-NT, 4-NT, 2,4-DNT and 2,6-DNT, or common organic solvents, was observed.

Qiu's group also tried to combine MOFs with other materials for the explosive detection.⁸² They present novel kinds of $\text{Fe}_3\text{O}_4@/\text{Tb-BTC}$ magnetic MOF nanospheres which possess both magnetic characteristics and fluorescent properties using a layer by layer assembly technique. It was applied in detection of nitroaromatic explosives, such as 2,4-dinitrotoluene (2,4-DNT), 2,6-dinitrotoluene (2,6-DNT), 2-nitrotoluene (2-NT), 4-nitrotoluene (4-NT), nitrobenzene (NB) and picric acid (PA). The results indicate that the fluorescence intensity of $\text{Fe}_3\text{O}_4@/\text{Tb-BTC}$ can be quenched by all analytes studied in the present work (Fig. 13). Remarkably, the as-synthesized

nanospheres exhibit high sensitivity for 2,4,6-trinitrotoluene (TNT) detection with K_{sv} value of (94800 M^{-1}) . Besides, the magnetic nanospheres can be easily recycled, which makes it more convenient for reutilization and friendly to the environment.

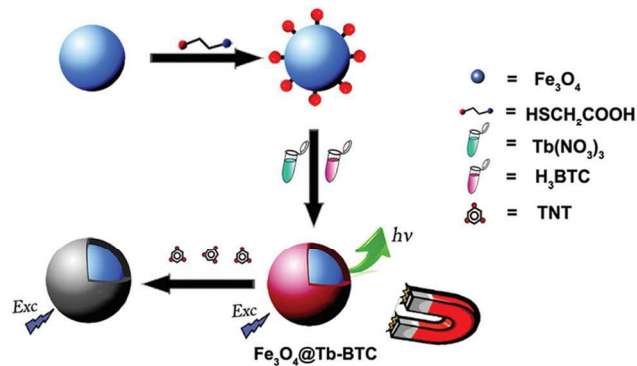


Fig. 13 Schematic illustration of the fabrication process of $\text{Fe}_3\text{O}_4@/\text{Tb-BTC}$ nanospheres. Reprinted with permission from ref 82. Copyright the Royal Society of Chemistry 2014.

Wang reported the successful preparation of a Mg-based luminescent MIL-53 MOF,⁶⁶ Desolvated this framework can be used as an absorbent for selective adsorption and separation of liquid explosives, including nitroaromatic (nitrobenzene (NB)) and nitroaliphatic (nitromethane (NM) and nitroethane (NE)) compounds, through single crystal-to-single crystal (SC-SC) transformations. On the basis of single crystal analysis, Wang provide direct evidence that both the selective adsorption and fluorescence quenching of the desolvated compound **1a** are dictated by host-guest interactions between guest liquid explosives and the host framework. Such findings differ from those reported in previous works, which were dominated by surficial close contact interactions (Fig. 14).

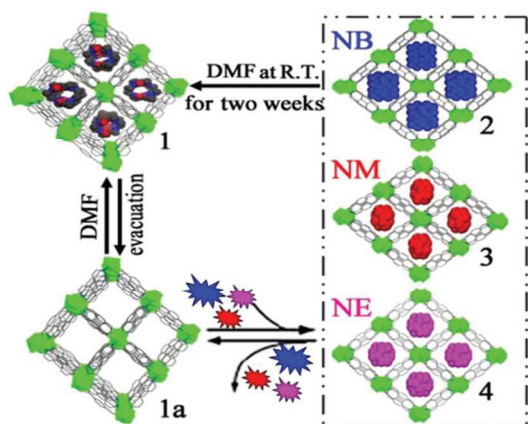


Fig. 14 Perspective views of the 3D open framework with 1D channel in 1 (with guest DMF molecules) and desolvated 1a; Reversibly selective adsorption of NB (2, in blue), NM (3, in red) and NE (4, in purple) by 1a; Crystals of 1 could be regenerated from 2, 3 and 4 by soaking them in DMF for two weeks at room temperature. Color code for 1: green, Mg; red, O; blue, N; 50% gray, C. Reprinted with permission from ref 66. Copyright the Royal Society of Chemistry 2014.

Mukherjee and coworkers reported three electron-rich MOFs by employing ligands bearing aromatic tags.²⁷ The key role of the chosen aromatic tags is to enhance the π -electron density of the luminescent MOFs. The study has revealed that all of these three prepared MOFs exhibited high selectivity towards explosive nitroaromatics such as DNT, TNT, and TNB over the other electron-deficient aromatics.

3. MOF Film for the NACs sensor

Many signal transduction schemes require a physical interface between the MOF and a device. This generally involves fabricating the MOF as a thin film on a surface. The increasing interest in utilizing MOFs as sensors or as selective membranes has led to a surge of interest in preparing MOF thin films.^{8a, 10}

Most commonly, MOF films have been synthesized directly on the surface of interest from the appropriate molecular and ionic precursors. Typically the surface is a metal, metal oxide, glass, or silicon. Film formation can sometimes be accomplished by simply placing a platform in a reactor with the

MOF precursors. These direct growth approaches often require functionalization of the surface with a self-assembled monolayer or seeding of the growth with small MOF crystals to nucleate film formation. In some cases, MOF films can be grown one molecular or ionic layer at a time by sequential immersions in solutions of the metal and organic precursors.¹⁰ These synthetic methods are typically multiple-step and time-consuming. Moreover, the substrate surfaces in these synthetic procedures need to be either electro-statically compatible or chemically modified upon pretreatment. Fransær and co-workers reported the flexibility of the electrochemical synthesis of MOFs films is illustrated by the preparation of well-adhering layers of luminescent MOFs on electrically conductive solid substrates (Fig. 15).⁸³ The luminescent layers have been successfully tested for the detection of 2,4-dinitrotoluene (DNT). Similarly A facile electrochemical plating method by means of applying voltage onto zinc electrodes in a BTC electrolyte has been developed to prepare fluorescent MOF films ($Zn_3(BTC)_2$).⁸⁴ Voltage and fabrication time are found to be the key parameters for the formation and morphology control of MOF films. Additionally, the as-prepared MOF films, due to their evident fluorescence, are explored for potential applications in detecting nitro explosives with detection limit as low as 0.5 ppm. The fluorescent MOF films can be further applied to distinguish nitro explosives by varying the solution concentration. Moreover, the MOF films exhibit excellent reusability in consecutive nitro explosive detection reactions.

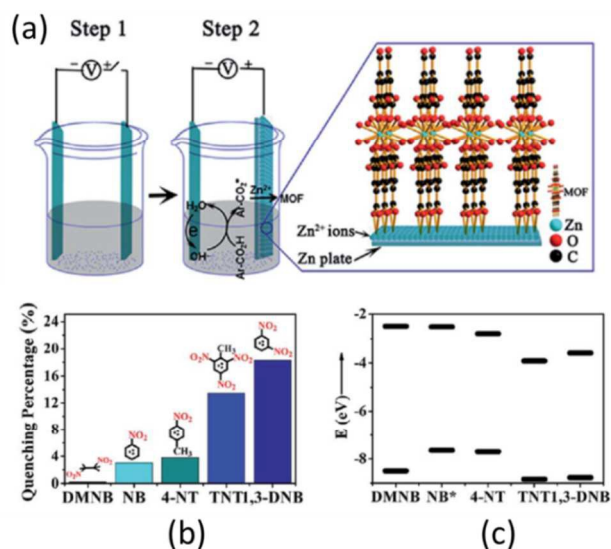


Fig. 15 (a) Schematic view of the preparation procedure of $Zn_3(BTC)_2$ MOF films; (b) quenching percentage of MOF films for different nitro explosive detection methods (0.5 ppm) in ethanol (excited and monitored at 327 nm and 362 nm, respectively); (c) theoretical HOMO and LUMO energies for some nitro explosives. Reprinted with permission from ref 84. Copyright the Royal Society of Chemistry 2014.

A second method for film fabrication is to first synthesize MOF particles and mixed them with other materials to obtain film. This has been demonstrated, for example, in Wen's work, thin films of Zn-MOF/PST-1 with a macroporous network structure were prepared by using electrospinning technique.⁸⁵ The secondary growth technique was developed to strongly anchor Zn-MOF seed crystals on porous supports Zn-MOF/PST-1 to form Zn-MOF/ PST-2 thin films. The MOF films of secondary growth have a good fluorescence quenching sensitivity to the nitroaromatic explosives such as dinitrotoluene(DNT), 2,4,6-trinitrotoluene(TNT), and thus can be good candidates for trace nitroaromatic explosives detection. Jaworski and Jung reported that nanocomposites containing azobenzoic acid functionalized graphene oxide and trans-4,4'-stilbene dicarboxylic acid in the presence of Zn^{2+} have been prepared with various ratios of the two components.⁸⁶ As shown in Fig. 16, the structure of the precursors is preserved in

the composites, where graphene layers from A-GO alternate with layers of MOF structures. The nanocomposites can act as chemosensors for DNT molecule detection.

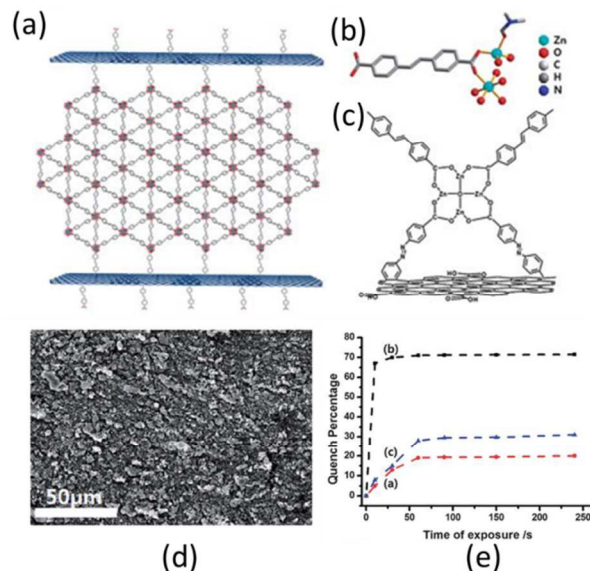


Fig. 16 (a) Schematic of the proposed bonding between $L-Zn^{2+}$ and A-GO- Zn^{2+} (b) The crystal structure of $L-Zn^{2+}$ showed two different coordination environments which have octahedral and tetrahedral coordination respectively. (c) Its simplified version. (d) Top view of SEM images of nanocomposite 1 layer of A-GO/ $L-Zn^{2+}$ (e) Fluorescence quenching of nanocomposite of A-GO/ $L-Zn^{2+}$ when exposed to (a) TNT and (b) DNT vapors. (c) Fluorescence quenching of pure crystal $L-Zn^{2+}$ when exposed to DNT vapor. Reprinted with permission from ref 86. Copyright the Royal Society of Chemistry 2013.

An unusual, but useful, third approach involves MOF film formation within the spatial constraints of a gel layer. Lee and Jung reported on the use of a fluorescent MOF hydrogel that exhibits a higher detection capability for TNT in the gel state compared with that in the solution state (Fig. 17).⁸⁷ A portable sensor prepared from filter paper coated by the hydrogel was able to detect TNT at the pictogram level with a detection limit of 1.82 ppt (parts per trillion). It presents a simple and new means to provide selective detection of TNT on a surface or in aqueous solution, as afforded by the unique molecular packing

through the MOF structure in the gel formation and the associated photophysical properties.

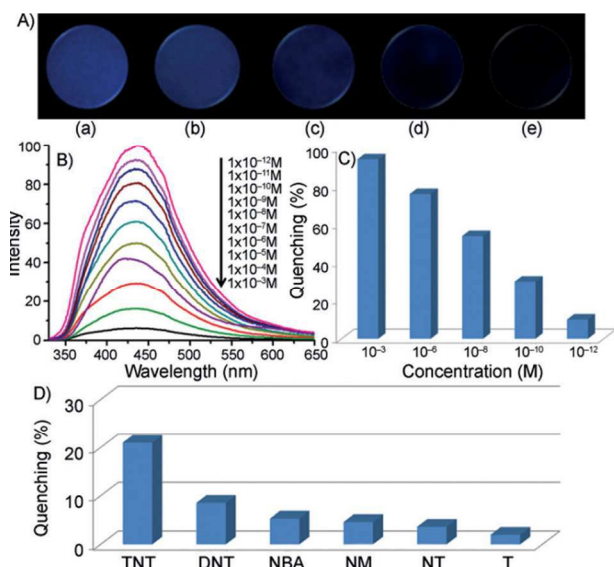


Fig. 17 (A) Photographs of the fluorescence quenching of gel 1-Zn²⁺-coated test strips by different concentration of TNT; (a) 0m, (b) 1.0×10⁻¹² M, (c) 1.0×10⁻¹⁰ M, (d) 1.0×10⁻⁸ M, and (e) 1.0×10⁻⁶ M; (B) Fluorescence spectral changes of the test strips on contact with added amount of TNT ($\lambda_{\text{ex}} = 302$ nm); (C) Plot of the quenching (%) against concentration of added TNT in acetonitrile; (D) Contact-mode detection of the lowest amount of different analytes 1.0×10⁻¹² M by the emission quenching test strip. Reprinted with permission from ref 87. Copyright the Wiley 2013.

4. Conclusions and outlook

In summary, we have briefly reviewed the recent research that is ongoing in the field of LMOFs for sensing NACs, including possible mechanisms for sensing. MOFs are intrinsic candidate for sensing, due to their luminescent and porous qualities, in which, water-stable LMOFs for NACs sensing is a potential development direction, because of the protection of environment and practical applications. As one of the most part of MOFs, it is supposed that the choice of metal ions is also worth discussing. Zn, Na, Mg and Zr ions can be exploited wildly instead of Cd and Ni ions. Hundreds of literatures have been reported about LMOFs for NACs sensing, but the study of LMOFs is a new research area. As for NACs, more obvious and simple signal changes can be obtained, such as color changes in

the range of visible light and “naked-eyes” detection. The advantage of LMOFs can also be taken through the post modification or composite with other materials. At the same time, it is much appreciated that preparing the device using stable and efficient MOF material makes the detection process simpler and easier. And it will be an important step in the development process of MOF material in NACs detection.

List of abbreviations

2,4-DNT	2,4-dinitrotoluene
2,6-DNT	2,6-Dinitrotoluene
H ₃ BTC	1,3,5-Benzenetricarboxylic acid
H ₃ CPEIP	5-((4-carboxyphenyl)ethynyl)isophthalic acid
HDMA	protonated dimethylamine cations
H ₂ L ¹	5-(benzyloxy)isophthalic acid
H ₂ L ²	5-(naphthalen-1-ylmethoxy)isophthalic acid
H ₂ L ³	5-(pyren-1-ylmethoxy)isophthalic acid
H ₄ L ⁴	bis-(3,5-dicarboxy-phenyl)terephthalamide
H ₄ L ⁵	1,1'-biphenyl-2,3,3',5'-tetracarboxylic acid
H ₂ L ⁶	3,3'-dimethoxybiphenyl-4,4'-dicarboxylic acid
H ₃ L ⁷	1,3,5-tris(4-carboxyphenyl-1-ylmethyl)-2,4,6-trimethylbenzene
H ₈ L ⁸	2,8,14,20-tetra-methyl-4,6,10,12,16,18,22,24-octacarboxymethoxy-calix[4]arene
H ₁₂ L ⁹	5,5',5'',5''',5]'-[1,2,3,4,5,6-phenylhexamethoxyl]hexaisophthalic acid
H ₃ L ¹⁰	2,4,6-tris[1-(3-carboxylphenoxy)ylmethyl]mesitylene
H ₂ L ¹¹	9,9-diethylfluorene-2,7-dicarboxylic acid
H ₈ L ¹²	tetrakis[(3,5-dicarboxyphenoxy)methyl] methane
H ₂ L ¹³	3,3'-(thiophene-2,5-diyl)dibenzoic acid
H ₄ L ¹⁴	1,1'-(1,4-phenylenebis(methylene))bis(1 <i>H</i> -pyrazole-3,5-dicarboxylic acid)
H ₄ L ¹⁵	[1,1':4',1''-terphenyl]-2',3,3'',5'-tetracarboxylic acid
H ₃ L ¹⁶	4,4',4''-(2,2',2''-(nitrilotris(methylene))tris(1 <i>H</i> -benzo[<i>d</i>]imidazole-2,1-diyl))tris(methylene))tribenzoic acid
H ₃ L ¹⁷	4,4',4''-(2,2',2''-(nitrilotris(methylene))tris(1 <i>H</i> -benzo[<i>d</i>]imidazole-2,1-diyl))tris(methylene))tribenzoic acid
H ₄ L ¹⁸	bis-(3,5-dicarboxy-phenyl)terephthalamide
H ₃ L ¹⁹	1,3,5-Tri(4-carboxyphenoxy)benzene
H ₂ L ²⁰	2-(2-Hydroxy-propionylamino)-terephthalic acid
H ₂ L ²¹	5-(4-carboxyphenyl)pyridine-2-carboxylat
H ₂ L ²²	2'-amino-[1,1':4',1''-terphenyl]-4,4''-dicarboxylic acid
H ₂ L ²⁴	H ₂ L ²⁴ = 2-phenylpyridine-5,4'-dicarboxylic acid
H ₂ bpdc	4,4'-biphenyldicarboxylic acid
H ₄ BPTA	[1,1'-biphenyl]-2,2',5,5'-tetracarboxylic acid
H ₃ BTB	1,3,5-benzenetrisbenzoic acid
H ₄ BTEC	1,2,4,5-benzenetetracarboxylic acid
H ₂ CPMA	bis(4-carboxyphenyl)- <i>N</i> -methylamine

ARTICLE

H ₂ DCPB	1,3-di(4-carboxyphenyl)benzene
Hdmp	3,5-dimethyl-4-(4'-pyridyl)pyrazole
H ₂ MFDA	9,9-dimethyl-fluorene-2,7-dicarboxylic acid
H ₃ NTB	4,4',4''-nitrotrisbenzoic acid
H ₂ oba	4,4'-oxybis(benzoic acid)
H ₂ PIA	5-(pyridine-4-yl)isophthalic acid
Htba	4-(1 <i>H</i> -1,2,4-triazol-1-yl)benzoic acid
H ₄ TCPE	tetrakis[4-(4-carboxyphenyl)phenyl]ethene
H ₃ TPT	<i>p</i> -terphenyl-3,4'',5-tricarboxylic acid
H ₄ ttac	1,1',2',1''-terphenyl-4,4',4'',5'-tetracarboxylic acid
H ₃ TTCA	Triphenylene-2,6,10-tricarboxylic acid
H ₃ TTPB	1,3,5-tri(4-(2 <i>H</i> -tetrazol-5-yl)phenoxy)benzene
ad	adenine
BDC	benzene-1,4-dicarboxylate
bimb	4,4'-bis(1-imidazolyl)biphenyl
bpe	1,2-bis(4-pyridyl)ethane
bpeb	1,4-bis[2-(4'-pyridyl)ethenyl]benzene
bpee	1,2-bis(4-pyridyl)ethylene
BPNO	4,4'-dipyridyl- <i>N,N'</i> -dioxide
bpp	1,3-bis(4-pyridyl)propane
BPTC	biphenyl-3,3',5,5'-tetracarboxylic acid
bpy	4,4'-bipyridine
bpydbH ₂	4,4'-(4,4'-bipyridine-2,6-diyl)dibenzoic acid
dcbpy	2,2'-bipyridine-4,4'-dicarboxylate
DEF	<i>N,N'</i> -diethylformamide
D-H ₂ cam	D-camphor acid
Diox	1,4-dioxane
dipb	4,4'-di(1 <i>H</i> -imidazol-1-yl)-1,10-biphenyl
DMA	<i>N,N'</i> -dimethylacetamide
DMF	<i>N,N'</i> -dimethylformamide
DMSO	Dimethyl sulphoxide
dpb	1,4-di(4-pyridyl)benzene
dpe	1,2-di(4-pyridyl)ethylene
dpyb	1,4-di(pyridin-4-yl)benzene
en	1,2-ethanediamine
fdc	2,5-furandicarboxylate dianion
IPA	isophthalic acid
G	guest solvent molecules
L ²³	4'-(4-methoxyphenyl)-4,2':6',4''-terpyridine
<i>m</i> -DNB	1,3-Dinitrobenzene
NB	Nitrobenzene
NDC	2,6-naphthalenedicarboxylic acid
NMP	1-methyl-2-pyrrolidone
NT	2-Nitrotoluene
PA	Picric acid
PAM	4,4'-methylenebis(3-hydroxy-2-naphthalenecarboxylate)
PCA	4-pyridinecarboxylic acid
<i>p</i> -DNB	1,4-Dinitrobenzene
ppvppa	<i>N</i> -(pyridin-2-yl)- <i>N'</i> -(4-(2-(pyridin-4-yl)vinyl)phenyl)pyridin-2-amine
PPZ	piperazine
sdb	4,4'-sulfonyldibenzoate
TATAB	4,4',4''-s-triazine-1,3,5-triyltri- <i>p</i> -aminobenzoate
TCA	tri-carboxytriphenylamine

TDPAT	2,4,6-tris(3,5-dicarboxyl phenylamino)-1,3,5-triazine
ted	triethylenediamine
TNT	2,4,6-trinitrotoluene
TPTZ	{4-[4-(1 <i>H</i> -1,2,4-triazol-1-yl)phenyl]phenyl}-1 <i>H</i> -1,2,4-triazole

Acknowledgements

This work was financially supported by the NSFC (Grant Nos. 21371179, 21271117), NCET-11-0309, the Shandong Natural Science Fund for Distinguished Young Scholars (JQ201003), and the Fundamental Research Funds for the Central Universities (13CX05010A, 14CX02150A, 14CX02158A).

Notes and references

State Key Laboratory of Heavy Oil Processing, China University of Petroleum (East China), College of Science, China University of Petroleum (East China), Qingdao Shandong 266580, People's Republic of China. E-mail: dfsun@upc.edu.cn

† These two authors provided equal contribution to this work.

- (a) S. W. Thomas III, G. D. Joly, and T. M. Swager, *Chem. Rev.*, 2007, **107**, 1339-1386; (b) D. T. McQuade, A. E. Pullen, and T. M. Swager, *Chem. Rev.*, 2010, **100**, 2537-2574; (c) A. Lan, K. Li, H. Wu, D. H. Olson, T. J. Emge, W. Ki, M. Hong and J. Li, *Angew. Chem., Int. Ed.*, 2009, **48**, 2334-2338; (d) M. E. Germain and M. J. Knapp, *Chem. Soc. Rev.*, 2009, **38**, 2543-2555; (e) Y. Salinas, R. Martinez-Manez, M. D. Marcos, F. Sancenon, A. M. Costero, M. Parra and S. Gil, *Chem. Soc. Rev.*, 2012, **41**, 1261-1296; (f) D. Banerjee, Z. Hu and J. Li, *Dalton Trans.*, 2014, **43**, 10668-10685; (g) S. Pramanik, C. Zheng, X. Zhang, T. J. Emge and J. Li, *J. Am. Chem. Soc.*, 2011, **133**, 4153-4155; (h) B. Liu, *J. Mater. Chem.*, 2012, **22**, 10094-10101; (i) S. J. Toal and W. C. Trogler, *J. Mater. Chem.*, 2006, **16**, 2871-2883; (j) L. Senesac and T. G. Thundat, *Mater. Today*, 2008, **11**, 28-36; (k) D. S. Moore, *Rev. Sci. Instrum.*, 2004, **75**, 2499-2512; (l) W. Wang, J. Yang, R. Wang, L. Zhang, J. Yu and D. Sun, *Cryst. Growth Des.*, 2015, **15**, 2589-2592; (m) K. S. Asha, K. Bhattacharyya and S. Mandal, *J. Mater. Chem. C*, 2014, **2**, 10073-10081.

2. S. Shanmugaraju and P. S. Mukherjee, *Chem.-Eur. J.*, 2015, **21**, 6656-6666.
3. (a) Z. Hu, B. J. Deibert and J. Li, *Chem. Soc. Rev.*, 2014, **43**, 5815-5840; (b) M.-M. Chen, X. Zhou, H.-X. Li, X.-X. Yang and J.-P. Lang, *Cryst. Growth Des.*, 2015, **15**, 2753-2760; (c) L. Liu, X. F. Chen, J. S. Qiu and C. Hao, *Dalton Trans.*, 2015, **44**, 2897-2906.
4. (a) V. P. Anferov, G. V. Mozjoukhine and R. Fisher, *Rev. Sci. Instrum.*, 2000, **71**, 1656-1659; (b) J. M. Sylvia, J. A. Janni, J. D. Klein, and K. M. Spencer, *Anal. Chem.*, 2000, **72**, 5834-5840; (c) K. Hakansson, R. V. Coorey, R. A. Zubarev, V. L. Talrose and P. Hakansson, *J. Mass Spectrom.*, 2000, **35**, 337-346; (d) S. F. Hallowell, *Talanta*, 2001, **54**, 447-458; (e) G. A. Eiceman, J. A. Stone, *Anal. Chem.*, 2004, **76**, 390A-397A; (f) Z. Takats, I. Cotte-Rodriguez, N. Talaty, H. Chen and R. G. Cooks, *Chem. Commun.*, 2005, 1950-1952; (g) R. D. Luggar, M. J. Farquharson, J. A. Horrocks and R. J. Lacey, *X-Ray Spectrom.*, 1998, **27**, 87-94
5. (a) S. Rochat and T. M. Swager, *ACS Appl. Mater. Interfaces*, 2013, **5**, 4488-4502; (b) J. C. Sanchez and W. C. Trogler, *J. Mater. Chem.*, 2008, **18**, 3143-3156.
6. (a) M. P. Suh, H. J. Park, T. K. Prasad and D. Lim, *Chem. Rev.*, 2012, **112**, 782-835; (b) R. B. Getman, Y. S. Bae, C. E. Wilmer and R. Q. Snurr, *Chem. Rev.*, 2012, **112**, 703-723; (c) J. R. Li, J. Scully and H. C. Zhou, *Chem. Rev.*, 2012, **112**, 869-932; (d) K. Sumida, D. L. Rogow, J. A. Mason, T. M. McDonald, E. D. Bloch, Z. R. Herm, T. H. Bae and J. R. Long, *Chem. Rev.*, 2012, **112**, 724-781; (e) Y. He, W. Zhou, G. Qian and B. Chen, *Chem. Soc. Rev.*, 2014, **43**, 5657-5678; (f) J. R. Li, R. J. Kuppler and H. C. Zhou, *Chem. Soc. Rev.*, 2009, **38**, 1477-1504; (g) B. Van de Voorde, B. Bueken, J. Denayer and D. De Vos, *Chem. Soc. Rev.*, 2014, **43**, 5766-5788.
7. (a) L. Ma, C. Abney and W. Lin, *Chem. Soc. Rev.*, 2009, **38**, 1248-1256; (b) M. Zhao, S. Ou and C. D. Wu, *Acc. Chem. Res.*, 2014, **47**, 1199-1207; (c) A. Dhakshinamoorthy and H. Garcia, *Chem. Soc. Rev.*, 2014, **43**, 5750-5765; (d) J. Lee, O. K. Farha, J. Roberts, K. A. Scheidt, S. T. Nguyen and J. T. Hupp, *Chem. Soc. Rev.*, 2009, **38**, 1450-1459; (e) J. Liu, L. Chen, H. Cui, J. Zhang, L. Zhang and C. Y. Su, *Chem. Soc. Rev.*, 2014, **43**, 6011-6061.
8. (a) L. E. Kreno, K. Leong, O. K. Farha, M. Allendorf, R. P. Van Duyne and J. T. Hupp, *Chem. Rev.*, 2012, **112**, 1105-1125; (b) Y. Cui, Y. Yue, G. Qian and B. Chen, *Chem. Rev.*, 2012, **112**, 1126-1162; (c) J. Rocha, L. D. Carlos, F. A. Paz and D. Ananias, *Chem. Soc. Rev.*, 2011, **40**, 926-940; (d) Y. Cui, B. Chen and G. Qian, *Coordin. Chem. Rev.*, 2014, 76-86.
9. R. C. Huxford, J. D. Rocca and W. Lin, *Curr. Opin. Chem. Biol.*, 2010, **14**, 262-268.
10. (a) H.-L. Jiang, T. A. Makal and H.-C. Zhou, *Coordin. Chem. Rev.*, 2013, **257**, 2232-2249; (b) Y. Chen, G. Li, Z. Chang, Y. Qu, Y. Zhang and X. Bu, *Chem. Sci.*, 2013, **4**, 3678-3682; (c) Y. Li, J. Li, L. Wang, B. Zhou, Q. Chen and X. Bu, *J. Mater. Chem. A*, 2013, **1**, 495-499.
11. K. Müller-Buschbaum, F. Beuerle and C. Feldmann, *Micropor. Mesopor. Mat.*, 2015, **216**, 171-199.
12. (a) S. S. Nagarkar, B. Joarder, A. K. Chaudhari, S. Mukherjee and S. K. Ghosh, *Angew. Chem., Int. Ed.*, 2013, **52**, 2881-2885; (b) J. R. Lakowicz, *Principles of Fluorescence spectroscopy*, Springer, Singapore, 3rd edn., 2010.
13. G. V. Zyryanov, D. S. Kopchuk, I. S. Kovalev, E. V. Nosova, V. L. Rusinov, O. N. Chupakhin, *Russ. Chem. Rev.*, 2014, **83**, 783-819.
14. B. Gole, A. K. Bar and P. S. Mukherjee, *Chem.-Eur. J.*, 2014, **20**, 2276-2291.
15. G.-Y. Wang, C. Song, D.-M. Kong, W.-J. Ruan, Z. Chang and Y. Li, *J. Mater. Chem. A*, 2014, **2**, 2213-2220.
16. Q. Zhang, A. Geng, H. Zhang, F. Hu, Z. H. Lu, D. Sun, X. Wei and C. Ma, *Chem.-Eur. J.*, 2014, **20**, 4885-4890.
17. D. Singh and C. M. Nagaraja, *Cryst. Growth Des.*, 2015, **15**, 3356-3365.
18. L. Sun, H. Xing, J. Xu, Z. Liang, J. Yu and R. Xu, *Dalton Trans.*, 2013, **42**, 5508-5513.
19. A.-X. Zhu, Z.-Z. Qiu, L.-B. Yang, X.-D. Fang, S.-J. Chen, Q.-Q. Xu and Q.-X. Li, *CrystEngComm*, 2015, **17**, 4787-4792.
20. C. Q. Zhang, Y. Yan, J. Y. Li, X. W. Song, Y. L. Liu and Z. Q. Liang, *Dalton Trans.*, 2015, **44**, 230-236.
21. C. Q. Zhang, Y. Yan, Q. H. Pan, L. B. Sun, H. M. He, Y. L. Liu, Z.

ARTICLE

- Q. Liang and J. Y. Li, *Dalton Trans.*, 2015, **44**, 13340-13346.
22. H. Xu, F. Liu, Y. Cui, B. Chen and G. Qian, *Chem. Commun.*, 2011, **47**, 3153-3155.
23. W. Sun, J. Wang, H. Liu, S. Chang, X. Qin and Z. Liu, *Mater. Lett.*, 2014, **126**, 189-192.
24. H. Zhang, D. M. Chen, H. L. Ma, and P. Cheng, *Chem.-Eur. J.*, 2015, DOI: 10.1002/chem.201502033, n/a-n/a.
25. J.-D. Xiao, L.-G. Qiu, F. Ke, Y.-P. Yuan, G.-S. Xu, Y.-M. Wang and X. Jiang, *J. Mater. Chem. A*, 2013, **1**, 8745-8752.
26. Y. N. Gong, L. Jiang and T. B. Lu, *Chem. Commun.*, 2013, **49**, 11113-11115.
27. B. Gole, A. K. Bar and P. S. Mukherjee, *Chem.-Eur. J.*, 2014, **20**, 13321-13336.
28. D. X. Ma, B. Y. Li, X. J. Zhou, Q. Zhou, K. Liu, G. Zeng, G. H. Li, Z. Shi and S. H. Feng, *Chem. Commun.*, 2013, **49**, 8964-8966.
29. Z. Zhang, S. Xiang, X. Rao, Q. Zheng, F. R. Fronczek, G. Qian and B. Chen, *Chem. Commun.*, 2010, **46**, 7205-7207.
30. Y. Kim, J. H. Song, W. R. Lee, W. J. Phang, K. S. Lim and C. S. Hong, *Cryst. Growth Des.*, 2014, **14**, 1933-1937.
31. Y. N. Gong, Y. L. Huang, L. Jiang and T. B. Lu, *Inorg. Chem.*, 2014, **53**, 9457-9459.
32. J. Ye, X. Wang, R. F. Bogale, L. Zhao, H. Cheng, W. Gong, J. Zhao and G. Ning, *Sensor. Actuat. B-Chem.*, 2015, **210**, 566-573.
33. J. Ye, L. Zhao, R. F. Bogale, Y. Gao, X. Wang, X. Qian, S. Guo, J. Zhao and G. Ning, *Chem.-Eur. J.*, 2015, **21**, 2029-2037.
34. X. Q. Wang, L. L. Zhang, J. Yang, F. L. Liu, F. N. Dai, R. M. Wang and D. F. Sun, *J. Mater. Chem. A*, 2015, **3**, 12777-12785.
35. T. K. Kim, J. H. Lee, D. Moon and H. R. Moon, *Inorg. Chem.*, 2013, **52**, 589-595.
36. Z.-F. Wu, B. Tan, M.-L. Feng, C.-F. Du and X.-Y. Huang, *J. Solid State Chem.*, 2015, **223**, 59-64.
37. Q. Zheng, F. Yang, M. Deng, Y. Ling, X. Liu, Z. Chen, Y. Wang, L. Weng and Y. Zhou, *Inorg. Chem.*, 2013, **52**, 10368-10374.
38. I. H. Park, R. Medishetty, J. Y. Kim, S. S. Lee and J. J. Vittal, *Angew. Chem., Int. Ed.*, 2014, **53**, 5591-5595.
39. D. Singh and C. M. Nagaraja, *Dalton Trans.*, 2014, **43**, 17912-17915.
40. H. He, Y. Song, F. Sun, Z. Bian, L. Gao and G. Zhu, *J. Mater. Chem. A*, 2015, **3**, 16598-16603.
41. H. Zhang, W. Jiang, J. Yang, Y.-Y. Liu, S. Song and J.-F. Ma, *CrystEngComm*, 2014, **16**, 9939-9946.
42. Y. C. He, H. M. Zhang, Y. Y. Liu, Q. Y. Zhai, Q. T. Shen, S. Y. Song, and J. F. Ma, *Cryst. Growth Des.*, 2014, **14**, 3174-3178.
43. M. Venkateswarulu, A. Pramanik, R. R. Koner, *Dalton Trans.*, 2015, **44**, 6348-6352.
44. D. Tian, Y. Li, R.-Y. Chen, Z. Chang, G.-Y. Wang and X.-H. Bu, *J. Mater. Chem. A*, 2014, **2**, 1465-1470.
45. L. L. Wen, X. Y. Xu, K. L. Lv, Y. M. Huang, X. F. Zheng, L. Zhou, R. Q. Sun, and D. F. Li, *ACS Appl. Mater. Interfaces*, 2015, **7**, 4449-4455.
46. Y. Wang, L. Cheng, Z. Y. Liu, X. G. Wang, B. Ding, L. Yin, B. B. Zhou, M. S. Li, J. X. Wang, and X. J. Zhao, *Chem.-Eur. J.*, 2015, **21**, 14171-14178.
47. H. He, Y. Song, F. Sun, N. Zhao and G. Zhu, *Cryst. Growth Des.*, 2015, **15**, 2033-2038.
48. D. Tian, R.-Y. Chen, J. Xu, Y.-W. Li and X.-H. Bu, *APL Materials*, 2014, **2**, 124111-124117.
49. X. Zhou, H. Li, H. Xiao, L. Li, Q. Zhao, T. Yang, J. Zuo and W. Huang, *Dalton Trans.*, 2013, **42**, 5718-5723.
50. A. Li, L. Li, Z. Lin, L. Song, Z. H. Wang, Q. Chen, T. Yang, X. H. Zhou, H. P. Xiao and X. J. Yin, *New J. Chem.*, 2015, **39**, 2289-2295.
51. X. H. Zhou, L. Li, H. H. Li, A. Li, T. Yang and W. Huang, *Dalton Trans.*, 2013, **42**, 12403-12409.
52. S.-N. Zhao, X.-Z. Song, M. Zhu, X. Meng, L.-L. Wu, S.-Y. Song, C. Wang and H.-J. Zhang, *RSC Adv.*, 2015, **5**, 93-98.
53. Y.-S. Xue, Y. He, L. Zhou, F.-J. Chen, Y. Xu, H.-B. Du, X.-Z. You and B. Chen, *J. Mater. Chem. A*, 2013, **1**, 4525-4530.
54. Z.-F. Wu, B. Tan, M.-L. Feng, A.-J. Lan and X.-Y. Huang, *J. Mater. Chem. A*, 2014, **2**, 6426-6431.
55. Z. W. J. Yang, K. L. Hu, Y. S. Li, J. F. Feng, J. L. Shi, and J. L. Gu, *ACS Appl. Mater. Interfaces*, 2015, **7**, 11956-11964.
56. Z. Q. Shi, Z. J. Guo and H. G. Zheng, *Chem. Commun.*, 2015, **51**, 8300-8303.

Journal Name

57. Y.-P. Xia, Y.-W. Li, D.-C. Li, Q.-X. Yao, Y.-C. Du and J.-M. Dou, *CrystEngComm*, 2015, **17**, 2459-2463.
58. Y. Wu, G.-P. Yang, Y. Zhao, W.-P. Wu, B. Liu and Y.-Y. Wang, *Dalton Trans.*, 2015, **44**, 3271-3277.
59. S. R. Zhang, D. Y. Du, J. S. Qin, S. J. Bao, S. L. Li, W. W. He, Y. Q. Lan, P. Shen, Z. M. Su, *Chem.-Eur. J.*, 2014, **20**, 3589-3594.
60. X. L. Hu, F. H. Liu, C. Qin, K. Z. Shao and Z. M. Su, *Dalton Trans.*, 2015, **44**, 7822-7827.
61. S. R. Zhang, D. Y. Du, J. S. Qin, S. L. Li, W. W. He, Y. Q. Lan and Z. M. Su, *Inorg. Chem.*, 2014, **53**, 8105-8113.
62. Y. Rachuri, B. Parmar, K. K. Bisht and E. Suresh, *Inorg. Chem. Front.*, 2015, **2**, 228-236.
63. X.-Z. Song, S.-Y. Song, S.-N. Zhao, Z.-M. Hao, M. Zhu, X. Meng, L.-L. Wu and H.-J. Zhang, *Adv. Funct. Mater.*, 2014, **24**, 4034-4041.
64. L.-Y. Pang, G.-P. Yang, J.-C. Jin, M. Kang, A.-Y. Fu, Y.-Y. Wang and Q.-Z. Shi, *Cryst. Growth Des.*, 2014, **14**, 2954-2961.
65. G. Y. Wang, L. L. Yang, Y. Li, H. Song, W. J. Ruan, Z. Chang and X. H. Bu, *Dalton Trans.*, 2013, **42**, 12865-12868.
66. Dan Liu, X. Liu, Y. Liu, Y. Yu, F. Chen and C. Wang, *Dalton Trans.*, 2014, **43**, 15237-15244.
67. A. K. Chaudhari, S. S. Nagarkar, B. Joarder and S. K. Ghosh, *Cryst. Growth Des.*, 2013, **13**, 3716-3721.
68. X. G. Liu, H. Wang, B. Chen, Y. Zou, Z. G. Gu, Z. Zhao and L. Shen, *Chem. Commun.*, 2015, **51**, 1677-1680.
69. D. Banerjee, Z. Hu, S. Pramanik, X. Zhang, H. Wang and J. Li, *CrystEngComm*, 2013, **15**, 9745-9750.
70. M. Jurcic, W. J. Peveler, C. N. Savory, D. O. Scanlon, A. J. Kenyone and I. P. Parkin *J. Mater. Chem. A*, 2015, **3**, 6351-6359.
71. B. Joarder, A. V. Desai, P. Samanta, S. Mukherjee and S. K. Ghosh, *Chem.-Eur. J.*, 2015, **21**, 965-969.
72. E.-L. Zhou, P. Huang, C. Qin, K.-Z. Shao and Z.-M. Su, *J. Mater. Chem. A*, 2015, **3**, 7224-7228.
73. J. H. Qin, B. Ma, X. F. Liu, H. L. Lu, X. Y. Dong, S. Q. Zang and H. W. Hou, *Dalton Trans.*, 2015, **44**, 14594-14603.
74. L.-H. Cao, F. Shi, W.-M. Zhang, S.-Q. Zang and T. C. W. Mak, *Chem.-Eur. J.*, 2015, DOI: 10.1002/chem.201501162, n/a-n/a.
75. J. H. Qin, B. Ma, X. F. Liu, H. L. Lu, X. Y. Dong, S. Q. Zang and H. W. Hou, *J. Mater. Chem. A*, 2015, **3**, 12690-12697.
76. S. S. Nagarkar, A. V. Desai, P. Samanta and S. K. Ghosh, *Dalton Trans.*, 2015, **44**, 15175-15180.
77. S. S. Nagarkar, A. V. Desai and S. K. Ghosh, *Chem. Commun.*, 2014, **50**, 8915-8918.
78. S. Mukherjee, A. V. Desai, B. Manna, A. I. Inamdar and S. K. Ghosh, *Cryst. Growth Des.*, 2015, **15**, 4627-4634.
79. W. Xie, S. R. Zhang, D. Y. Du, J. S. Qin, S. J. Bao, J. Li, Z. M. Su, W. W. He, Q. Fu and Y. Q. Lan, *Inorg. Chem.*, 2015, **54**, 3290-3296.
80. S. Khatua, S. Goswami, S. Biswas, K. Tomar, H. S. Jena and S. Konar, *Chem. Mater.*, 2015, **27**, 5349-5360.
81. R. Li, Y. P. Yuan, L. G. Qiu, W. Zhang and J. F. Zhu, *Small*, 2012, **8**, 225-230.
82. J. J. Qian, L. G. Qiu, Y. M. Wang, Y. P. Yuan, A. J. Xie and Y. H. Shen, *Dalton Trans.*, 2014, **43**, 3978-3983.
83. N. Campagnol, E. R. Souza, D. E. De Vos, K. Binnemans and J. Fransaer, *Chem. Commun.*, 2014, **50**, 12545-12547.
84. Y.-Y. Yang, Z.-J. Lin, T.-T. Liu, J. Liang and R. Cao, *CrystEngComm*, 2015, **17**, 1381-1388.
85. Y. Xu, Y. Wen, W. Zhu, Y.-n. Wu, C. Lin and G. Li, *Mater. Lett.*, 2012, **87**, 20-23.
86. J. H. Lee, J. Jaworski and J. H. Jung, *Nanoscale*, 2013, **5**, 8533-8540.
87. J. H. Lee, S. Kang, J. Y. Lee, J. Jaworski and J. H. Jung, *Chem.-Eur. J.*, 2013, **19**, 16665-16671.